Optimal Energy Management Strategy for a Hybrid Vehicle provided with a Dual Electric Storage System

Thomas Miro Padovani, Guillaume Colin, Ahmed Ketfi-Cherif, Yann Chamaillard

Optimal Energy Management Strategy for a Hybrid Vehicle provided with a Dual Electric Storage System

Thomas MIRO PADOVANI * **Guillaume COLIN** **
Ahmed KETFI-CHERIF * **Yann CHAMAILLARD** **

* *Renault SAS, France, (e-mail: {Thomas.Miro-Padovani, Ahmed.Ketfi-Cherif}@renault.com)*
** *Laboratoire PRISME, Université d'Orléans, France, (e-mail: {guillaume.colin, yann.chamaillard}@univ-orleans.fr)*

Abstract: This paper addresses the energy management problem of a Mild hybrid electric vehicle (HEV) provided with a singular dual electric storage system. The latter is the combination of a Li-ion battery, a double layer capacitor (DLC) pack and a DC/DC converter. The energy management of the hybrid powertrain is formulated as an optimal control problem with two dimensional control and state variables. The optimal solution is computed using deterministic dynamic programming (DDP), and an on-line oriented solution based on the equivalent consumption minimization strategy (ECMS) is proposed. Simulation results of both strategies are presented and discussed, highlighting the minor sub-optimality of the on-line energy management strategy (EMS).

Keywords: Energy management strategy, Optimal control, Hybrid electric vehicle, Dual storage system, Pontryagin's Minimum Principle.

1. INTRODUCTION

Hybrid electric vehicles (HEVs) and Plug-in hybrid electric vehicles (PHEVs) are currently among the most promising solutions to maximize global powertrain efficiency and therefore reduce the fuel consumption of our vehicles. Powertrain hybridization opens the way to an almost unlimited set of solutions in terms of architectures, technologies and sizing, each leading to a different compromise. The main feature of the powertrain discussed in this paper comes from its electric storage system. While the electric storage system of most HEVs is made of a single Li-ion or Ni-MH battery pack, this paper focuses on a singular architecture, composed of a 12V Li-ion battery associated in series with a pack of double layer capacitors (DLC). Energy transfer between the two devices is performed by a bi-directional DC/DC converter. The main motivation behind this architecture is to combine the high specific power and durability of the DLC with the high specific energy of Li-ion batteries. With an appropriate supervisory control, this system can lead to reduced energy losses while enhancing battery life span. The work in this paper aims at proposing an embeddable energy management strategy (EMS) for the studied Mild-HEV, based on optimal control theory, and taking into account both storage devices.

Optimal control theory has been widely investigated to provide both off-line and on-line oriented solutions for the HEV energy management problem. Off-line strategies such as deterministic dynamic programming (DDP) Sunström et al. (2008); Lin et al. (2003); Elbert et al. (2013) and Pontryagin's Minimum Principle (PMP) require the knowledge of future driving conditions to achieve optimality. On the other hand, on-line strategies need to be causal, and while they can be implemented in a vehicle, optimality is no longer guaranteed. The most common optimal-control based on-line strategies are stochastic dynamic programming (SDP) Moura et al. (2011); Kolmanovsky et al. (2002) and the Equivalent Consumption Minimization Strategy (ECMS) Paganelli et al. (2002); Chasse et al. (2010), which is the on-line counterpart of the PMP.

Dual storage systems embedded in vehicular applications have already been addressed in previous work Romaus et al. (2009); Allegre et al. (2009); Cheng and Wismer (2007); Omar et al. (2010). The work presented in this paper differs from the singular electric architecture considered where the 12V battery is a part of both the 12V and the high voltage (HV) traction grid. Moreover, the optimization of the dual storage system is encompassed in the traditional HEV energy management problem by considering an extra state variable similarly to Fontaine et al. (2013). Both the off-line optimal solution and an on-line oriented solution are presented and discussed. The powertrain architecture and models are presented in section 2. The optimal control problem dealing with both storage devices is presented in section 3. In section 4, optimal results yielded through DDP are discussed. Finally, an application of the ECMS for the dual storage system is proposed in section 5, and the results are discussed and compared to the DDP optimal solution.

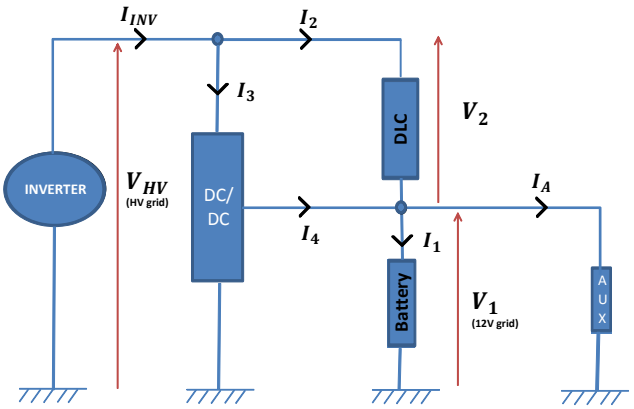

Fig. 1. Electrical diagram of the dual storage system considered.

Table 1. Vehicle characteristics.

Vehicle mass	1500 kg
Engine displacement	1.5 L
Engine maximum power	80 kW
Electric machine maximum power	12 kW
Combined energy storage capacity	200 Wh

2. VEHICLE SPECIFICATIONS AND MODELS

2.1 Vehicle architecture

The vehicle considered in this paper is a parallel Mild-HEV, provided with a 12 kW belt-driven starter generator connected to the crankshaft of a 1.5 L turbo diesel engine producing 80 kW. The engine is connected to a 6 gear manual transmission. The main innovation in the powertrain comes from its electric storage system, composed of two storage devices connected in series: a 12V Li-ion battery pack and a 36V DLC pack. Both storage devices in series make the high voltage (HV) grid (48V), therefore both devices contribute to traction power. The 12V battery pack is connected to the HV grid via a bi-directional DC/DC converter. Finally, the inverter supplying the electric machine (EM) is connected to the HV grid. Both storage devices offer a combined usable electric energy of approximately 200 W.h.
Fig. 1 illustrates the electrical diagram of the architecture as well as the naming convention for currents and voltages in the system. The singularity of this topology, where the 12V battery belongs to both the 12V grid and the HV grid, logically results in a strong coupling between the two grids of the vehicle. Consequently, the power consumption of the inverter P_{INV} will directly impact the 12V grid through the battery; similarly the power consumption P_A of the auxiliaries on the 12V grid will impact the available power for the EM. The main powertrain and vehicle characteristics are listed in table 1.

2.2 Powertrain and vehicle models

The model used for simulation is a control-oriented backward quasi-static model. The speed profile is given by a driving cycle which provides both the vehicle speed $v(t)$ and acceleration setpoint. The vehicle model computes the corresponding required powertrain torque at the wheel T^{sp}_{pwt} as follows:

$$T^{sp}_{pwt}(t) = (m_{veh}.\dot{v}(t) + F_{res}(t) + F_{brk}(t) + m_{veh}.g.\sin(\alpha(t))).r_{wheel}, \quad (1)$$

with m_{veh} the vehicle mass, F_{brk} the force applied by the braking system, α the slope angle, g the gravitational acceleration, and r_{wheel} the wheel radius. F_{res} is the resistive force applied to the vehicle caused by the rolling friction and drag. It is modeled by a second order polynomial:

$$F_{res}(t) = p_1.v^2(t) + p_2.v(t) + p_3, \quad (2)$$

where p_{1-3} are identified via the experimental road load given by the deceleration law of the considered vehicle.
The manual transmission model provides the rotary speed of the internal combustion engine (ICE) and EM, ω_{ICE} and ω_{EM}, given the wheel speed ω_{wheel}:

$$\begin{aligned} \omega_{ICE} &= Rgb(g_{nbr}).\omega_{wheel} \\ \omega_{EM} &= R_{EM}.\omega_{ICE}, \end{aligned} \quad (3)$$

where $Rgb(g_{nbr})$ expresses the gearbox ratio corresponding to the gear number g_{nbr} and R_{EM} is the constant gear ratio between the crankshaft and EM.
The engine consumption $\dot{m}_{fuel}$ is computed using a look-up table given by experimental results on an engine test bench in nominal operating conditions:

$$\dot{m}_{fuel} = f_{ICE}(\omega_{ICE}, T_{ICE}). \quad (4)$$

The dynamics on the torque are ignored, and T_{ICE} the output torque of the ICE exactly matches the torque setpoint given by the EMS.
The EM electrical power P_{INV} is given by a look-up table based on dynamometer testing,

$$P_{INV} = f_{EM}(\omega_{EM}, T_{EM}), \quad (5)$$

where T_{EM} is the output torque of the EM. As for the ICE, the EM's dynamics is ignored and T_{EM} matches a given valid setpoint.
To ensure that the driver torque demand is always met, the EM torque and ICE torque are linked by the following:

$$T_{pwt} = (T_{ICE} + T_{EM}.R_{EM}).Rgb(g_{nbr}) = T^{sp}_{pwt}. \quad (6)$$

The battery and DLC pack are modeled as an open circuit voltage (OCV) source associated with an internal resistance R in series, both depending on the battery state of energy (SoE):

$$S_v : \begin{cases} V_1 = OCV_1(SoE) + R_1(SoE).I_1 \\ V_2 = OCV_2(SoE) + R_2(SoE).I_2 \\ V_{HV} = V_1 + V_2, \end{cases} \quad (7)$$

with V_1 and V_2 the battery and DLC voltages. As a convention, the index 1 refers to battery-related quantities, and 2 refers to the DLC.
The bi-directional DC/DC converter is modeled as follows:

$$P_C = V_1.I_4 = \eta_C.V_{HV}.I_3, \quad (8)$$

with

$$\eta_C = \begin{cases} \eta & \text{if } P_C \geq 0 \\ \dfrac{1}{\eta} & \text{else,} \end{cases} \quad (9)$$

where η is a constant approximation of the DC/DC efficiency. The auxiliaries power consumption P_A is considered as a known constant perturbation.
Finally, the electrified part of the powertrain presented in Fig. 1 can be modeled from Kirchhoff's laws with the following system of equations:

$$S : \begin{cases} V_1.I_4 = \eta_C.V_{HV}.I_3 \ ; \ I_A = \dfrac{P_A}{V_1} \\ I_{INV} = \dfrac{P_{INV}}{V_{HV}} \quad ; \ P_C = V_1.I_4 \\ I_2 = I_{INV} - I_3 \quad ; \ I_1 = I_4 + I_2 - I_A, \end{cases} \tag{10}$$

where as a convention, a positive power or current will result in charging the storage devices. S can be reduced to a system with 3 equations and 3 unknowns, namely I_3, I_2 and I_1:

$$S_I : \left\{ I_3 = \frac{P_C}{\eta_C.V_{HV}};\ I_2 = \frac{P_{INV}}{V_{HV}} - I_3;\ I_1 = \frac{P_C - P_A}{V_1} + I_2. \right. \tag{11}$$

When incorporating the expressions of the voltages in S_v into the system of equations S_I, one obtains a nonlinear system of second degree equations with no simple analytical solution. The difficulty of the system comes from the coupling between voltages and currents, coming from the internal resistance of the storage devices. In order to break the algebraic constraint between the computation of currents and voltages, a fixed point method is proposed. For the first step, we assume as initial conditions $R_1 = R_2 = 0$, allowing us to replace V_1 and V_{HV} in S_I by respectively OCV_1 and $OCV_1 + OCV_2$. This assumption leads to a first estimation of the currents in S_I. These current estimations are used to compute the voltages in S_v, which are in turn used to compute a better estimation of the currents in S_I. By repeating the process, one iteratively computes a more precise estimation of the currents in S_I. Once the currents converge with a successive error below 1%, the corresponding solution is selected. For the electrical system considered here, a maximum of 5 iterations was enough to meet the convergence criterion of a 1% error or less.

Once the 3 currents of S_I are known, it is possible to calculate the dynamics of both storage devices' SoE by integrating their inner power P^{inn} over time:

$$\dot{SoE}_j(SoE_j, t) = \frac{P_j^{inn}}{E_j} = \frac{OCV_j(SoE).I_j(t)}{E_j}, \tag{12}$$

where $j = \{1, 2\}$ depending on the considered device, E_j is the battery or DLC available energy when fully charged, and P_j^{inn} is the inner battery or DLC power.

3. OPTIMAL CONTROL PROBLEM FORMULATION

Optimal control based EMS require the definition of an optimality criterion, also called performance index, which serves as the control policy's objective. The performance index considered in this paper is the global fuel consumption along the trip:

$$\begin{aligned} J(\mathbf{x}(t), \mathbf{u}(t)) &= \int_{t_0}^{t_f} \dot{m}_{fuel}(\mathbf{u}(t), t).dt + \Phi\left(\mathbf{x}(t_f)\right) \\ \mathbf{u}_{opt} &= \underset{\mathbf{u}}{\operatorname{argmin}}\, J(\mathbf{x}(t), \mathbf{u}(t)) \end{aligned} \tag{13}$$

with

$$\Phi\left(\mathbf{x}(t_f)\right) = \begin{cases} 0 & \text{if } \mathbf{x}(t_f) \geq \mathbf{SoE}_{target} \\ \infty & \text{else.} \end{cases} \tag{14}$$

The control variable $\mathbf{u}$ is chosen as follows:

$$\mathbf{u} = \begin{Bmatrix} u_1 \\ u_2 \end{Bmatrix} = \begin{Bmatrix} P_C \\ P_{INV} \end{Bmatrix}. \tag{15}$$

The considered state variable $\mathbf{x}$ is made of both storage devices' SoE:

$$\mathbf{x} = \begin{Bmatrix} x_1 \\ x_2 \end{Bmatrix} = \begin{Bmatrix} SoE_1 \\ SoE_2 \end{Bmatrix}, \tag{16}$$

$\Phi\left(\mathbf{x}(t_f)\right)$ is a function ensuring that the solution meets the final requirement on both SoEs. The final SoEs, namely $\mathbf{SoE}_{target}$, will be chosen equal to their initial values to ensure sustaining operation. The optimization problem (13) is subject to :

$$\begin{cases} \mathbf{u}(t) \in \boldsymbol{\mathcal{U}}(t) \\ \mathbf{x}(t) \in \boldsymbol{\chi} \\ \dot{x}_1(t) = f_1(x_1(t), \mathbf{u}(t), t), x_1(t_0) = x_{1,0} \\ \dot{x}_2(t) = f_2(x_2(t), \mathbf{u}(t), t), x_2(t_0) = x_{2,0}, \end{cases} \tag{17}$$

where $\boldsymbol{\mathcal{U}}(t)$ is the set of admissible commands for P_{INV} and P_C. Likewise, χ is the space of admissible values for both state variables.

The two state functions f_1 and f_2 are given by :

$$\begin{aligned} f_1(x_1(t), \mathbf{u}(t), t) &= \frac{OCV_1(x_1(t)).I_1(x_1(t), \mathbf{u}(t), t)}{E_1}, \\ f_2(x_2(t), \mathbf{u}(t), t) &= \frac{OCV_2(x_2(t)).I_2(x_2(t), \mathbf{u}(t), t)}{E_2}. \end{aligned} \tag{18}$$

with the expression of I_1 and I_2 given by (11).

One of the distinctive features of the optimal control problem presented lies in the calculation of the set of admissible commands $\boldsymbol{\mathcal{U}}(t)$. In addition to regular limitations on the actuators:

$$\begin{matrix} \underline{P}_{INV} & \leq P_{INV} & \leq \overline{P}_{INV} \\ \underline{P}_C & \leq P_C & \leq \overline{P}_C, \end{matrix} \tag{19}$$

where $\underline{X}$ and $\overline{X}$ denote respectively the minimum and maximum admissible values for X. Battery and DLC power limitations must be taken into consideration:

$$\begin{matrix} \underline{P}_1 \leq P_1 \leq \overline{P}_1 \\ \underline{P}_2 \leq P_2 \leq \overline{P}_2, \end{matrix} \tag{20}$$

Battery and DLC power limitations are needed to ensure that the optimal commands yielded by the EMS will be accepted by the battery management system (BMS), and therefore will not deteriorate the storage devices. Power limitations may also be used to ensure a set of voltage limitations, for instance on the 12V grid.

As a result, 4 inequality constraints are considered to determine the final set of admissible commands $\boldsymbol{\mathcal{U}}(t)$:

$$\begin{cases} \underline{P}_C \leq & P_C & \leq \overline{P}_C \\ \underline{P}_{INV} \leq & P_{INV} & \leq \overline{P}_{INV} \\ \underline{P}_2.C_2 \leq & P_{INV} - \dfrac{1}{\eta_C}.P_C & \leq \overline{P}_2.C_2 \\ (\underline{P}_1 + P_A).C_1 \leq & P_{INV} + (C_1 - \dfrac{1}{\eta_C}).P_C & \leq (\overline{P}_1 + P_A).C_1, \end{cases} \tag{21}$$

with

$$C_1 = \frac{V_{HV}}{V_1}, \qquad C_2 = \frac{V_{HV}}{V_2}. \tag{22}$$

The inequality constraints corresponding respectively to the DC/DC, inverter, DLC, and battery power limitations are expressed via (11) and (19). The inequalities system (21) takes the general formulation:

$$\begin{cases} \underline{u_1} \leq & u_1 & \leq \overline{u_1} \\ \underline{u_2} \leq & u_2 & \leq \overline{u_2} \\ \underline{z} & \leq u_2 + \alpha.u_1 & \leq \overline{z} \\ \underline{w} & \leq u_2 + \beta.u_1 & \leq \overline{w}, \end{cases} \tag{23}$$

with in this case $\alpha < 0$ and $\beta > 0$. From (23), one can determine global limitations on u_2 versus u_1 :

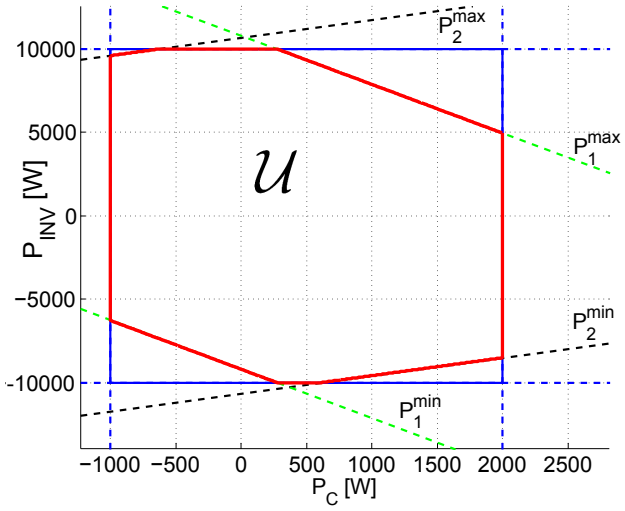

Fig. 2. Depiction of the 2 dimensional space of admissible commands $\boldsymbol{\mathcal{U}}$ for the considered optimal control problem.

$$\max(\underline{u_2}, \underline{z}-\alpha.u_1, \underline{w}-\beta.u_1) \leq u_2 \leq \min(\overline{u_2}, \overline{z}-\alpha.u_1, \overline{w}-\beta.u_1) \tag{24}$$

Eq. (24) gives a set of 9 inequalities, 6 of which are relevant to define the absolute limitations on u_1:

$$\max(\underline{u_1}, \frac{\underline{w}-\overline{u_2}}{\beta}, \frac{\overline{z}-\underline{u_2}}{\alpha}, \frac{\underline{w}-\overline{z}}{\beta-\alpha}) \leq u_1 \leq \min(\overline{u_1}, \frac{\overline{w}-\underline{u_2}}{\beta}, \frac{\underline{z}-\overline{u_2}}{\alpha}, \frac{\underline{z}-\overline{w}}{\alpha-\beta}). \tag{25}$$

Finally, with (25) giving the global limitations on u_1 ensuring the set of constraints (23), and with (24) giving the global limitations on u_2 versus u_1, the set of admissible commands $\boldsymbol{\mathcal{U}}(t) \in (u_1, u_2)$ is defined. Fig. 2 plots $\boldsymbol{\mathcal{U}}(t)$ for nominal operating conditions. The numerical values considered for this example are the following:

$$\begin{array}{lll} -10000 \leq P_{INV} \leq 10000, & -1000 \leq P_C \leq 2000 \\ -2500 \leq P_1 \leq 2500, & -8000 \leq P_2 \leq 8000 \end{array} \tag{26}$$

The domain corresponding to the actuators' limitations is represented by the blue lines. The green dashed lines represent the controls reaching the minimum and maximum battery power limitations, whereas DLC power limitations are represented in black. The set of admissible commands is the intersection of all previously mentioned domains, and is represented in red. Determining a priori the space of admissible controls rather than eliminating non-feasible commands a posteriori has two main advantages. Not only does it ensure feasible commands, but it also reduces the search area of the control space to what is necessary only during the minimization process, reducing the computational burden for vehicle embedded applications.

4. OFF-LINE OPTIMAL SOLUTION

The optimal control problem (13) presented in section 3 is solved using DDP. Commonly, the EMS problem only considers one state variable corresponding to the single storage device present. The extra state variable considered in this paper greatly increases the computational effort required by the DDP to solve the problem. However, computational time remain reasonable for off-line computer based simulations; mainly because the very low levels of battery energy considered require a smaller number of points to properly discretize the state space.

Fig. 3 and 4 present the optimal solution for the Worldwide harmonized Light duty driving Test Cycle (WLTC) considering 250 W of auxiliaries' power consumption and charge sustaining operation. When analyzing the optimal control policy, several interesting behaviors can be identified. First of all regarding the DC/DC converter, the reversibility of the latter is never used, as swapping energy back and forth between storage devices leads to unnecessary losses when all the driving conditions are perfectly known a priori. Therefore the DC/DC converter is only used to charge the 12V battery, strictly to compensate for the auxiliaries power consumption. The optimal control policy of the DC/DC converter shows that the instantaneous power $P_C(t)$ is either null or close to the maximum efficiency of the converter. However, the mean value of $P_C(t)$) along the entire driving cycle is always equal to the mean value of the auxiliaries' consumption.

As for the P_{INV} command, it is worth noting that for this specific powertrain, using the EM to optimize the ICE's operating point is not optimal. The EM power and efficiency are not high enough to justify operating point optimization for the diesel engine which has a large area of flat specific fuel consumption. As a result, the EM is used as a generator only when the electric energy recovered during deceleration phases is not enough to compensate for the auxiliaries' consumption.

When analyzing the impact of the optimal control policy on the storage devices, it appears clearly that the EMS avoids high battery currents. Indeed, during deceleration phases when the EM produces its maximum levels of power, the DC/DC power goes back to 0 to avoid overcharging the battery, cf Fig 3. Symmetrically, during engine starts where the EM requires a lot of power, the DC/DC converter is used to relieve the battery by lowering its discharge current. The EMS always favors using the DC/DC to avoid too high values for $|I_1|$, even if it means increasing $|I_2|$. This comes from the fact that R_1 is substantially higher than R_2, the battery is therefore more subject to ohmic losses. Avoiding high battery current is also very important to preserve the battery state of Health (SoH), as it also reduces battery temperature and overall A.h throughput, which are the three main factors aggravating battery aging Miro-Padovani et al. (2013).

Finally, when analyzing both SoEs, the DLC clearly serve as the main energy buffer, whereas SoE_1 remains almost constant, as shown in Fig. 4. Moreover, SoE_2 is highly correlated to vehicle speed: the optimal EMS always ensures depletion between two deceleration phases to guarantee sufficient available energy storage for each deceleration phase. Therefore, SoE_2 is in average higher at low speed than it is at high speed.

5. PROPOSED ON-LINE STRATEGY

To solve the optimal control problem (13) on-line, an extended version of the well-known ECMS taking into account two state variables is proposed. The PMP states that the optimal policy $\mathbf{u}_{opt}(t)$ has to minimize, for all $t \in [t_0; t_f]$, the following Hamiltonian function:

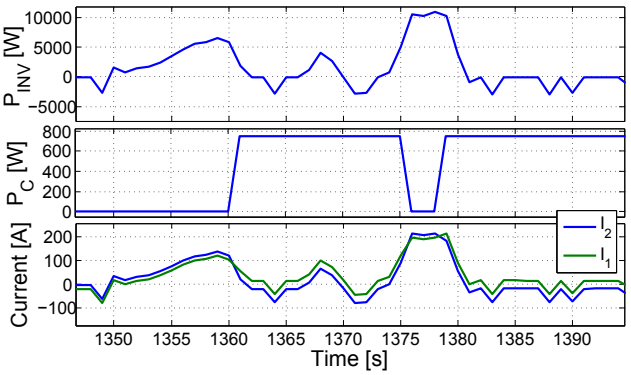

Fig. 3. Zoom on optimal control trajectory during deceleration phases. When P_{INV} is high, P_C remains null to avoid increasing the battery current.

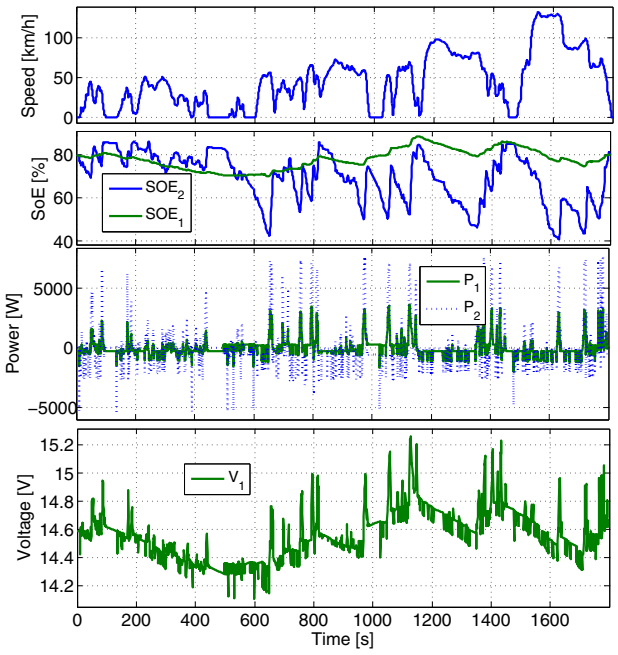

Fig. 4. Optimal solution yielded by DP for the WLTC cycle.

$$\begin{aligned} H(\mathbf{u},\boldsymbol{\lambda},\mathbf{x},t) &= \dot{m}_{fuel}(u_1,t)+\lambda_1(t).\dot{x}_1(\mathbf{u},x_1,t) \\ &\quad +\lambda_2(t).\dot{x}_2(\mathbf{u},x_2,t) \\ H_{eq}(\mathbf{u},\mathbf{s},\mathbf{x},t) &= \dot{m}_{fuel}(u_1,t).H_{LHV}-s_1(t).P_1^{inn}(\mathbf{u},x_1,t) \\ &\quad -s_2(t).P_2^{inn}(\mathbf{u},x_2,t), \end{aligned} \tag{27}$$

with

$$\mathbf{s}(t)=\left\{\begin{array}{c} s_1(t) \\ s_2(t) \end{array}\right\}=\left\{\begin{array}{c} \dfrac{-\lambda_1(t).H_{LHV}}{E_1} \\ \dfrac{-\lambda_2(t).H_{LHV}}{E_2} \end{array}\right\}, \tag{28}$$

where $\boldsymbol{\lambda}(t)=\left\{\begin{array}{c}\lambda_1(t)\\ \lambda_2(t)\end{array}\right\}$ is the co-state vector, and the low heating value of the fuel H_{LHV} is used to express the fuel consumption as a power consumption. $\mathbf{s}(t)$ dictates the equivalent fuel cost of the battery and DLC inner power P_1^{inn} and P_2^{inn}. The dynamics of $\mathbf{s}(t)$ is given by the Euler-Lagrange equation:

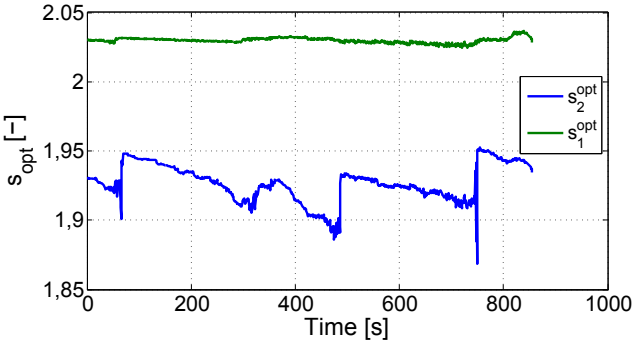

Fig. 5. Optimal values of $\mathbf{s}(t)$ calculated with DDP on the Artemis urban cycle.

$$\dot{\mathbf{s}}(t)=-\frac{\partial H_{eq}(.)}{\partial \mathbf{x}} \tag{29}$$

However, $\mathbf{s}(t)$ is commonly considered constant since for Li-ion batteries $\frac{\partial \dot{\mathbf{x}}(.)}{\partial \mathbf{x}}$ is close to 0 for a large range of SoE. This assumption is verified here by calculating the optimal values of $s_1(t)$ and $s_2(t)$ using DDP, cf Fig. 5, as the co-state of the dual problem is given by:

$$\boldsymbol{\lambda}(t)=\frac{\partial}{\partial \mathbf{x}}V_{opt}(\mathbf{x}(t),t), \tag{30}$$

where $V_{opt}(.)$ is the optimal-value, or cost-to-go function considered in Bellman's principle Elbert et al. (2013).
The simulation results presented in this section were obtained considering an on-line adaptation of $s_1(t)$ and $s_2(t)$ via a proportional-integral controller of the SoE for each:

$$s_j(t)=s_0^j+K_p^j.SoE_{err}^j+K_i^j.\int_{t_0}^{t}SoE_{err}^j.dt \tag{31}$$

with

$$SoE_{err}^j=SoE_{target}^j-SoE_j(t) \tag{32}$$

where $j=\{1,2\}$ and the parameters s_0^j, K_p^j, and K_i^j are kept unique for every driving cycle. Therefore they are chosen in order to obtain a global robustness on the SoE regulation for all driving conditions, especially to ensure that the SoEs remain bounded within the state constraints domain $\boldsymbol{\chi}$. Readers can refer to Chasse et al. (2010) for more information on equivalence factor tuning methods. While an on-line adaptation of s_1 and s_2 using a PI controller is by nature sub-optimal, it is essential to prevent both SoEs from diverging when driving conditions are not known a priori.
Fig. 6 presents simulation results given by the proposed on-line strategy on the WLTC cycle with $P_A = 250$W. Several differences appear regarding the optimal solution presented Fig 3 and 4. While the DC/DC is mainly used to charge the 12V battery, here it is also used in reverse mode a few times to ensure robustness of the SoE_2 regulation. Moreover, SoE_2 is no longer correlated with vehicle speed, as the proposed on-line strategy does not anticipate future acceleration or deceleration phases. Apart from these items, all of the behaviors discussed in section 4 are common to the optimal solution and the on-line strategy presented.
The sub-optimality results of the on-line strategy are given in table 2 for different driving cycles and accessories consumption. The sub-optimality is defined as the relative extra fuel consumption regarding the optimal DDP solu-

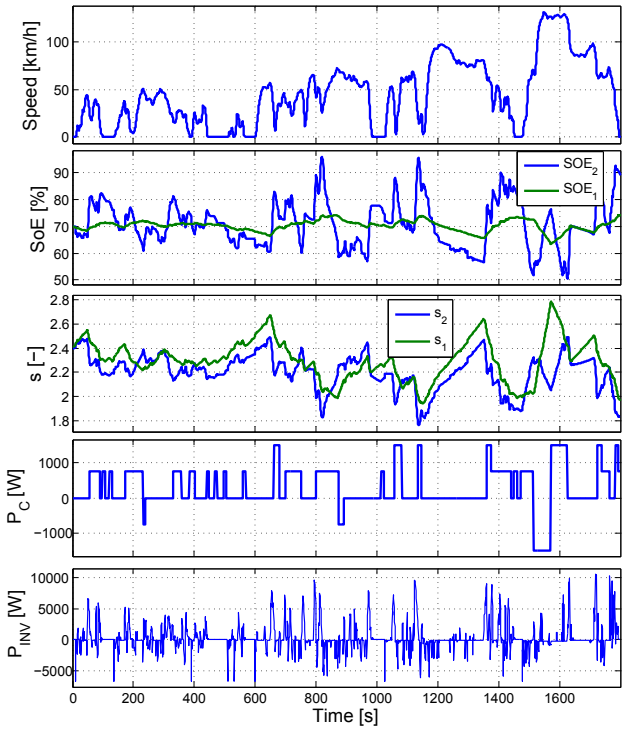

Fig. 6. On-line strategy results on the WLTC cycle.

Table 2. Extra fuel consumption of the on-line strategy relative to the optimal solution.

Extra fuel consumption [%]				
P_A [W]	WLTC	Urban	Extra-urban	Traffic jam
250	0.7	0.4	0.5	0.4
600	1	1.3	0.7	1.7
900	1.2	1.8	0.8	2.8

tion. The driving cycles considered are the WLTC and the Artemis cycles. The cycles were repeated ten times in a row, in order to ensure that the possible energy unbalance between $\mathbf{x}(t_0)$ and $\mathbf{x}(t_f)$ of a few W.h was absolutely negligible regarding the total fuel mass consumed. Overall, the extra fuel consumption yielded by the on-line strategy did not exceed 2.8%, it even remained below 1% for $P_A = 250$ W. But most importantly, these results were obtained with a single set of tuning parameters for the SoE regulators, highlighting the potential of the ECMS strategy to give near-optimal results with a good overall robustness and a low tuning effort.

6. CONCLUSION

Dual storage systems are viable solutions for electrified powertrains to combine the advantages of different technologies or to benefit from the energy stored in the traditional 12V battery. The system presented in this paper combines a 12V Li-ion battery with a DLC pack, both devices in series forming the HV traction grid. Energy transfer between the 12V and HV grids is ensured by a bi-directional DC/DC converter. The electric system is modeled and the algebraic constraint resulting in the coupling of voltages and currents is solved through a fixed point method. The energy management of the HEV powertrain is formulated as an optimal control problem considering two control variables and two state variables. A mathematical approach is presented to define the space of admissible controls taking into account actuators and storage devices power limitations. The optimal control problem is solved off-line using DDP, and the main results of the optimal solution are discussed. Although the optimal solution's only target is to minimize fuel consumption, it also preserves the battery SoH by avoiding high currents. High currents are the main cause of energy losses via the joule effect, and at the same time a factor aggravating battery aging. Finally, an on-line EMS based on the ECMS is presented, taking into account the two state variables with a double co-state formulation. The strategy shows very promising simulation results, yielding a fuel consumption very close to the optimal solution for the considered system in all experimented situations. The overall robustness of the strategy is one of its main assets, as all the simulations were conducted with a single set of tuning parameters.

REFERENCES

Allegre, A.L., Bouscayrol, A., and Trigui, R. (2009). Influence of control strategies on battery/supercapacitor hybrid energy storage systems for traction applications. In *IEEE Vehicle Power and Propulsion Conference*, 213–220. USA.

Chasse, A., Sciarretta, A., and Chauvin, J. (2010). Online optimal control of a parallel hybrid with costate adaptation rule. In *Proceedings of the 2010 IFAC Symposium Advances in Automotive Control*.

Cheng, D.L. and Wismer, M.G. (2007). Active control of power sharing in a battery/ultracapacitor hybrid source. In *IEEE Conference on Industrial Electronics and Applications*, 2913–2918. China.

Elbert, P., Ebbesen, S., and Guzzella, L. (2013). Implementation of dynamic programming for n-dimensional optimal control problems with final state constraints. *IEEE Transactions on Control Systems Technology*, 21(3), 924–931.

Fontaine, C., Delprat, S., Paganelli, S., and Guerra, T. (2013). Optimal control of a parallel hybrid vehicle equipped with a dual electrical storage system. In *Proceedings of the 2010 IFAC Symposium Advances in Automotive Control*. Japan.

Kolmanovsky, I., Siverguina, I., and Lygoe, B. (2002). Optimization of powertrain operating policy for feasibility assessment and calibration: Stochastic dynamic programming approach. In *Proceedings of the 2002 American Control Conference*. USA.

Lin, C.C., Peng, H., Grizzle, J., and Kang, J.M. (2003). Power management strategy for a parallel hybrid electric truck. *IEEE Transactions on Control Systems Technology*, 11(6), 839–849.

Miro-Padovani, T., Debert, M., Colin, G., and Chamaillard, Y. (2013). Optimal energy management strategy including battery health through thermal management for hybrid vehicles. In *Proceedings of the 2013 IFAC Symposium Advances in Automotive Control*. Japan.

Moura, S.J., Fathy, H.K., Callaway, D.S., and Stein, J.L. (2011). A stochastic optimal control approach for power management in plug-in hybrid electric vehicles. *IEEE Transactions on Control Systems Technology*, 19, 545–555.

Omar, N., Mierlo, J.V., Verbrugge, B., and den Bossche, P.V. (2010). Power and life enhancement of battery-electrical double layer capacitor for hybrid electric and charge-depleting plug-in vehicle applications. *Electrochimica Acta*, 55(25), 7524–7531.

Paganelli, G., Delprat, S., Guerra, T., Rimaux, J., and Santin, J. (2002). Equivalent consumption minimization strategy for parallel hybrid powertrains. In *Proceedings of 55th IEEE Vehicular technology conference*. USA.

Romaus, C., Bocker, J., Seifried, K.W.A., and Znamenshchykov, O. (2009). Optimal energy management for a hybrid energy storage system combining batteries and double layer capacitors. In *IEEE Energy Conversion Congress and Exposition*, 1640–1647. USA.

Sunström, O., Guzzella, L., and Soltic, P. (2008). Optimal hybridization in two parallel hybrid electric vehicles using dynamic programming. In *Proceedings of 17th World Congress The International Federation of Automatic Control Seoul*. Korea.